IOP PUBLISHING SCIENCE AND TECHNOLOGY OF ADVANCED MATERIALS

Sci. Technol. Adv. Mater. **12** (2011) 055003 (6pp) doi:10.1088/1468-6996/12/5/055003

Effect of sintering temperature on optical properties and microstructure of translucent zirconia prepared by high-pressure spark plasma sintering

Haibin Zhang, Byung-Nam Kim, Koji Morita, Hidehiro Yoshida Keijiro Hiraga and Yoshio Sakka

Advanced Materials Processing Unit, National Institute for Materials Science, 1-2-1 Sengen, Tsukuba, Ibaraki 305-0047, Japan

E-mail: ZHANG.Haibin@nims.go.jp

Received 20 May 2011
Accepted for publication 19 July 2011
Published 7 September 2011
Online at stacks.iop.org/STAM/12/055003

Abstract

Aiming to characterize the effect of sintering temperature on transparency of zirconia, we have evaluated the optical properties and microstructure of translucent cubic zirconia prepared by high-pressure spark plasma sintering (SPS) at 1000–1200 °C. Color centers (oxygen vacancies with trapped electrons) and residual pores were primary defects in the samples. In SPS samples, the total forward transmittance and in-line transmittance are mainly affected by color centers with a limited contribution from residual pores; in contrast, the changes in reflectance are only related to the porosity. The amounts of color centers and residual pores increase with sintering temperature that reduces the total forward and in-line transmittance of the as-sintered zirconia. Annealing in oxidizing atmosphere improves the total forward and in-line transmittance. During the annealing, the concentration of color centers decreases but the porosity increases.

Keywords: translucent zirconia, optical materials, spark plasma sintering, optical properties

1. Introduction

Cubic yttria-stabilized zirconia (c-YSZ) is an important structural/functional ceramic with existing and potential applications, such as solid electrolyte for fuel cells and oxygen sensors. Recently, polycrystalline transparent zirconia has attracted increasing attention because of its unique combination of mechanical and optical properties [1–12]. For high density and good transparency, transparent polycrystalline c-YSZ is usually prepared with hot-isostatic pressing (HIP) [7, 8]. However, high sintering temperatures of HIP produce large grains in the resultant specimens [6–8]. This deteriorates mechanical properties, which are important not only for mechanical but also for optical applications of c-YSZ.

To restrain grain growth, spark plasma sintering (SPS) is used as an alternative method to prepare transparent c-YSZ [9–12], as well as other transparent ceramics, such as Al_2O_3 [13–22], $MgAl_2O_4$ [23–27], $Y_3Al_5O_{12}$ [27–29], MgO [30] and $3Al_2O_3 \cdot 2SiO_2$ [31,32]. Garay and co-workers [9, 10] reported that nanograined transparent c-YSZ could be produced by SPS at a moderate pressure of 141 MPa. Munir and co-workers [11] and the present authors [12] demonstrated that the application of high pressure during SPS enhances the transparency of c-YSZ. The coupling of SPS with high pressure is effective for preparing other transparent ceramics too, such as alumina [33].

Our recent research demonstrated [12] that sintering temperature is crucial for the transparency of c-YSZ, and that the optimum sintering temperature is 1100 °C [12]. To

elaborate this parameter, in this work, we investigated the effect of sintering temperature during the high-pressure SPS processing on the microstructure and optical properties of the translucent c-YSZ.

2. Experimental details

2.1. Specimen preparation

Commercial 8 mol% Y_2O_3-ZrO_2 powders (TZ-8Y, Tosoh Corporation, Tokyo, Japan) were employed as the starting material. The powders were consolidated using an SPS machine (SPS-1050, SPS Syntex Inc. Kawasaki, Japan) in vacuum (10^{-3} Torr) to obtain dense bulk specimens. In this study, the applied pressure and heating rate were respectively fixed to 400 MPa and 10 °C min^{-1}. The sintering temperature ranged from 1000 to 1200 °C, as monitored by an optical pyrometer focused on the non-through hole (1 mm diameter and 2 mm depth) in the graphite die. Heating was conducted using a sequence consisting of 12 dc pulses (40.8 ms) with the interval of 6.8 ms. The details of the high-pressure SPS process can be found elsewhere [12]. Sintering resulted in disk samples of 10 mm diameter and 1.3 mm thickness.

2.2. Optical characterization

For measuring optical properties, both surfaces of the as-prepared disks were mirror-polished using diamond slurry. The total forward transmittance, in-line transmittance and reflection were measured with a double-beam spectrophotometer (SolidSpec-3700DUV, Shimazu Co Ltd, Kyoto, Japan) equipped with an integrating sphere. The distance between the sample and the detector was about 55 cm. For in-line transmittance measurements, a 3 mm pinhole was placed in front of the detector selecting only the in-line transmitted portion of the incident light (5 mm diameter). This setup allowed us to measure the 'real in-line transmittance' [34].

The absorption coefficients C_{abs} of the specimens were calculated using the measured reflection (R) and total forward transmittance (T) as

$$C_{abs} = -\frac{\ln \frac{T}{1-R}}{t}, \tag{1}$$

where t is the sample thickness.

The scattering coefficients γ_{sca} were calculated from the total forward transmittance (T) and in-line transmittance (I) as

$$\gamma_{sca} = -\frac{\ln \frac{I}{T}}{t}. \tag{2}$$

2.3. Microstructure observation

The grain size was measured using a scanning electron microscope (SEM, JSM-6500, JEOL) by evaluating the average cross-sectional area per grain under the assumption of spherical grains. The measured grain size was an apparent one, so it was multiplied by 1.225 to determine the true grain size.

For transmission electron microscope (TEM) observations, a 500 μm-thick slab was cut by a low-speed diamond cutter, mechanically polished down to 100 μm, and further thinned with an Ar ion-milling machine. The TEM observations were performed using a JEOL-2010F microscope (JEOL Ltd, Akishima, Tokyo, Japan) operated at 200 kV. Because the samples had small pores and low porosity, grain boundary grooving caused by etching would distort the SEM images. Therefore, the porosity was measured by TEM, as an average value over five images.

2.4. Annealing

To characterize the effect of annealing on the optical properties, the SPS samples were heated in a furnace at 900 °C for 4 h in air. The optical properties were compared before and after annealing.

2.5. Simulation of pore scattering effect on optical properties

Light scattering by pores was simulated using the computation code *BHMIE* [7, 11, 20, 22], which is based on the Mie scattering theory and is widely used to model scattering phenomena in transparent ceramics [7, 11, 20, 22]. The assumptions of *BHMIE* were (i) homogenous distribution of monodisperse pores, (ii) no reflection on sample surfaces and (iii) no absorption.

3. Results and discussions

Figure 1 shows the appearance of the as-sintered and annealed c-YSZ. The specimen sintered at 1000 °C is opaque owing to insufficient densification. Increasing temperature up to or above 1075 °C results in yellowish-brown, transparent c-YSZ, and the samples progressively darken with increasing sintering temperature.

The yellowish-brown appearance of c-YSZ is usually attributed to color centers (oxygen vacancies with trapped electrons) [9–12], [35–37], which are easily produced in c-YSZ under thermal reduction or electroreduction conditions [9–12], [35–39]. The SPS process provides both conditions: at high temperatures, vacuum and graphite dies yield a thermal reduction environment, and the applied current may also result in electroreduction. This is the reason of the easy formation of color centers in SPS zirconia [9–12].

The formation of oxygen vacancies in c-YSZ due to reduction can be expressed using the standard Kröger–Vick notation as

$$O_O^{\times} = \tfrac{1}{2} O_2 + V_O^{\bullet\bullet} + 2e'. \tag{3}$$

These oxygen vacancies can cause strong light absorption through the association with free electrons to form color centers [9–12], [35–37], [39]. The oxygen vacancies with one trapped electron are F^+ centers and the ones with two trapped electrons are F centers.

$$V_O^{\bullet\bullet} + e' = V_O^{\bullet} \quad (F^+), \tag{4}$$

$$V_O^{\bullet\bullet} + 2e' = V_O^{\times} \quad (F). \tag{5}$$

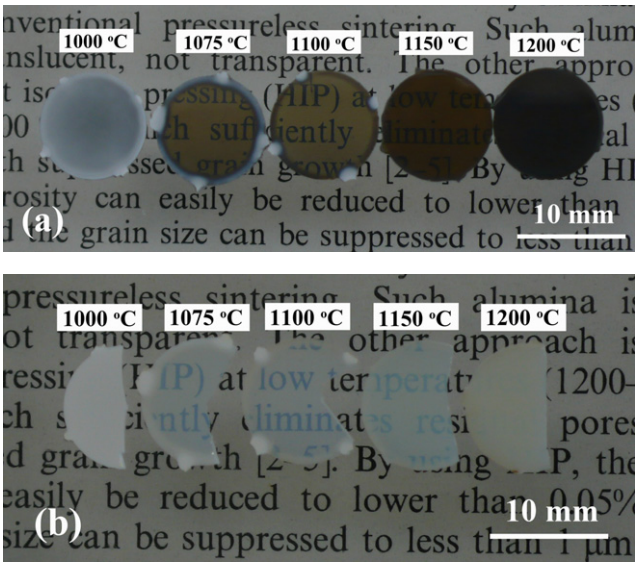

Figure 1. Photographs of (a) yttria stabilized zirconia disks produced by SPS at 1000 to 1200 °C for 10 min under a pressure of 400 MPa and (b) the same samples after annealing treatment. The samples had a thickness of 1 mm and were placed 30 mm above the text.

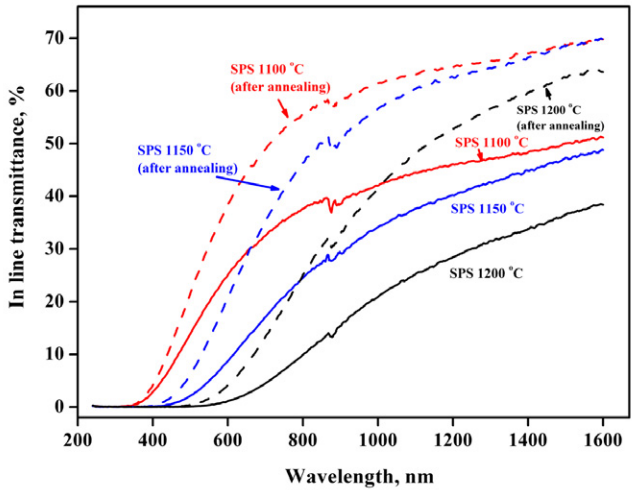

Figure 2. Typical in-line transmittance spectra of the as-sintered (solid line) and annealed c-YSZ (dashed line). The data were normalized for a thickness of 1 mm. The optical properties were similar for the samples prepared at 1075 and 1100 °C, thus we restricted our measurements to the samples sintered at ⩾ 1100 °C.

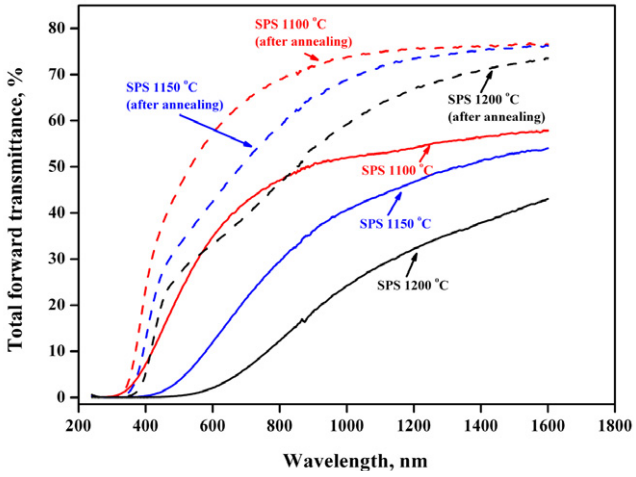

Figure 3. Typical total forward transmittance spectra of the as-sintered (solid line) and annealed c-YSZ (dashed line). The data were normalized for a thickness of 1 mm.

These color centers result in strong absorption and the yellowish-brown coloration (figure 1(a)). Obviously, the amount of color centers increases with sintering temperature because of a harsher reduction environment that results in darker samples (figure 1(a)).

On the other hand, annealing in oxidizing atmosphere can diffuse oxygen back and reduce color centers [10–12]. Hence it can be seen that upon annealing the sample color lightens to milky white (figure 1(b)).

Figures 2 and 3, respectively, show typical in-line transmittance and total forward transmittance spectra of c-YSZ sintered between 1100 and 1200 °C. They reveal that (i) higher sintering temperature results in lower transparency (in-line transmittance and total forward transmittance) for both the as-sintered and annealed c-YSZ, and that (ii) the annealing dramatically improves both the in-line and total forward transmittance of the as-sintered c-YSZ.

Besides color centers, residual pores reduce transparency of c-YSZ, especially for the ultraviolet light (figures 2 and 3) [7,12,20], [39–41]. Figure 4 shows typical TEM microstructures of the as-sintered polycrystalline c-YSZ. It can be seen that small intergranular pores are surrounded by grains. In addition, the grain sizes of the samples are sensitive to the preparation condition and increase with sintering temperature. Also, the amount of residual pores increases with sintering temperature and the pore size remains nearly constant. The dependence of the grain size and porosity on sintering temperature is shown in figure 5.

Thus the transparency of the as-sintered c-YSZ is influenced by both the color centers and residual pores, which respectively contribute to absorption (figure 6) and scattering (figure 7). As the sintering temperature is raised, the absorption and scattering coefficients increase for both the as-sintered and annealed specimens that accounts for the decrease of transparency above 1100 °C (figures 2 and 3).

Absorption and scattering are affected differently by annealing (figures 6 and 7). The absorption coefficient is reduced (figure 6) because back-diffusion of oxygen reduces the concentration of color centers [10–12]. However, the color centers can coalesce and eventually develop into pores [12,36,39]. So the scattering coefficient is enhanced (figure 7) owing to the increase of the porosity (figure 5).

Usually the pore scattering significantly affects the transparency of ceramics [13–32]. However, annealing experiments on SPS samples indicate only a weak effect of residual pores on transparency [10–12]. The porosity is relatively low for SPS samples because the application of high pressure effectively improves the densification (figure 5). Meanwhile, the residual pores are very fine (30–40 nm) owing to the use of nanopowders as the starting material (figure 4). In contrast, the reduced condition of SPS generates high concentration of color centers [10–12]. As a result, absorption

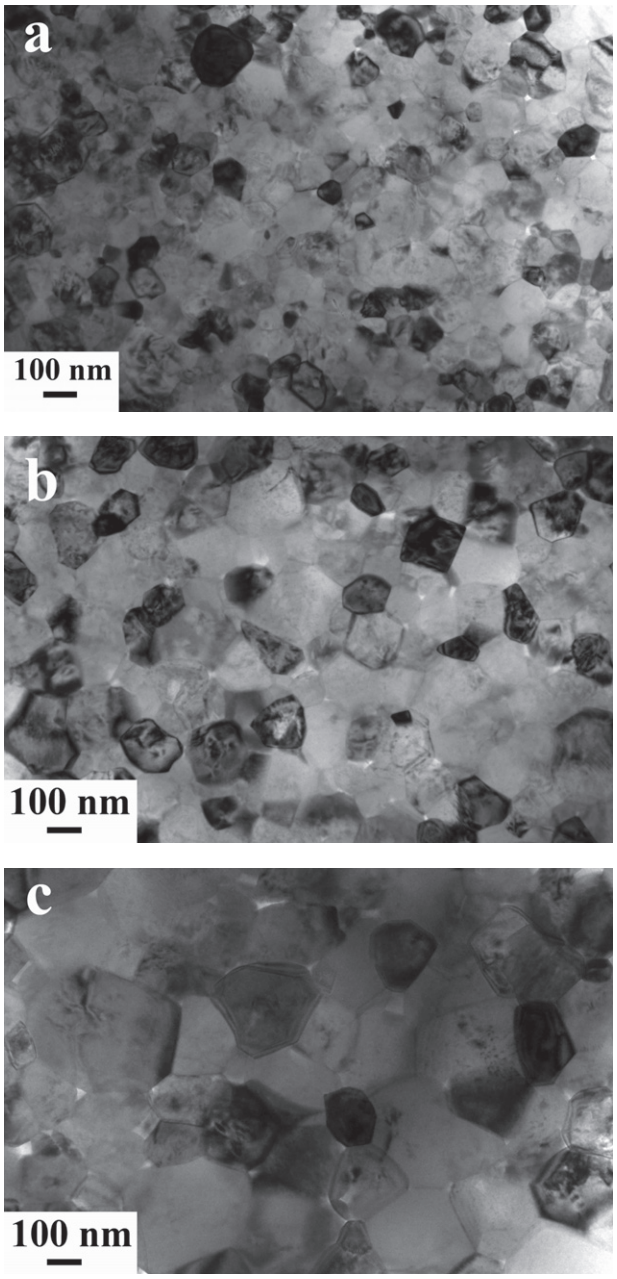

Figure 4. Bright-field TEM images of c-YSZ sintered at (a) 1100 °C, (b) 1150 °C and (c) 1200 °C.

from color centers has much more significant effect on the transparency of the as-sintered c-YSZ than scattering from residual pores [10–12]. Therefore, although light scattering is enhanced by the increase of the porosity (figure 7), the overall transparency is still considerably improved by annealing (figures 2 and 3) owing to the removal of color centers (figure 6).

Residual pores dominate the transparency of the annealed specimens since most color centers have been removed and converted into pores. Accordingly, the decrease of total forward and in-line transmittance of the annealed c-YSZ (figures 2 and 3) with sintering temperature can be attributed to the increase of porosity (figure 5).

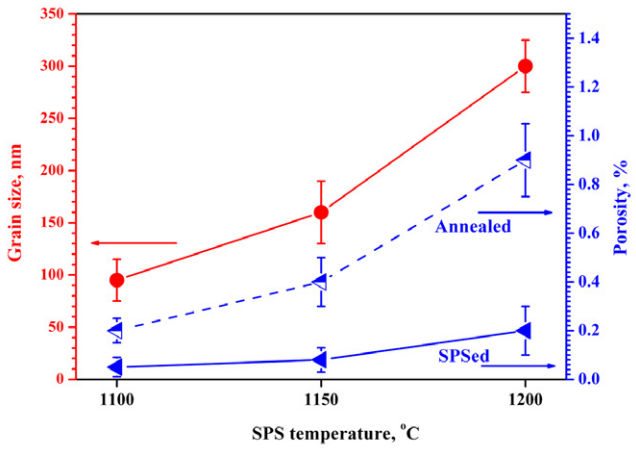

Figure 5. Dependence of the grain size and porosity on the sintering temperature.

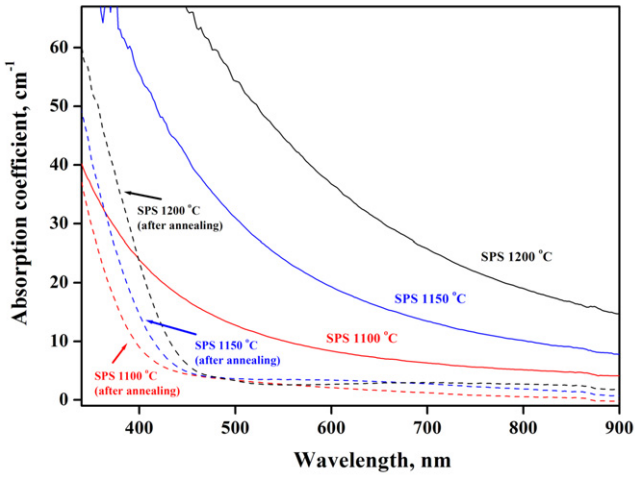

Figure 6. Absorption coefficients of the as-sintered (solid line) and annealed c-YSZ (dashed line) as a function of the sintering temperature.

Figure 8 shows the dependence of light reflection on sintering temperature. The reflection is similar for as-sintered samples; it is strongly enhanced after annealing, and the effect is more pronounced for higher sintering temperature. The measured value consists of the intrinsic reflection at the front and back surfaces of the sample and scattering from the residual pores. Since the intrinsic reflection is independent of sintering temperature, the variation of the measured reflection is only related to the porosity change. The as-sintered samples have similar reflection because of their similar porosity (figure 5). The porosity is increased by annealing that results in higher reflection values. In addition, the reflection maximum shifts towards longer wavelengths with increasing sintering temperature. This phenomenon is also attributed to the increase of porosity, as confirmed by the theoretical calculation (figure 9) using a dedicated computer program *BHMIE* [7, 11, 20, 22] (see figure 9). Note that changing the pore size in simulation can not reproduce the experimentally observed intensity trend.

Figure 10 shows a typical high-resolution TEM image of the grain boundaries in the annealed c-YSZ. Amorphous or

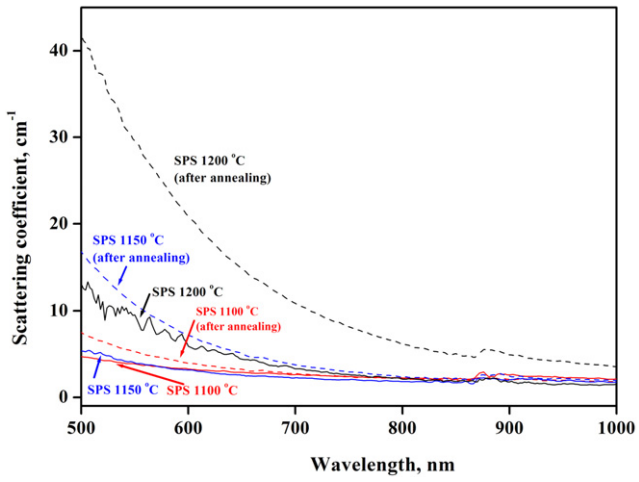

Figure 7. Scattering coefficients of the as-sintered (solid line) and annealed c-YSZ (dashed line) as a function of the sintering temperature.

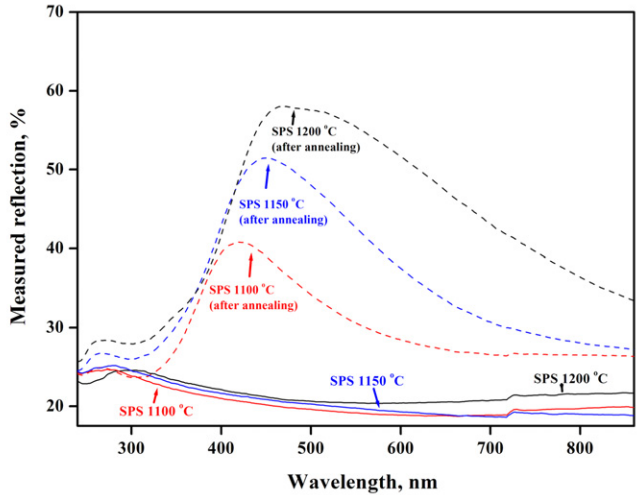

Figure 8. Dependence of the measured reflection on sintering temperature for the as-sintered (solid line) and annealed c-YSZ (dashed line).

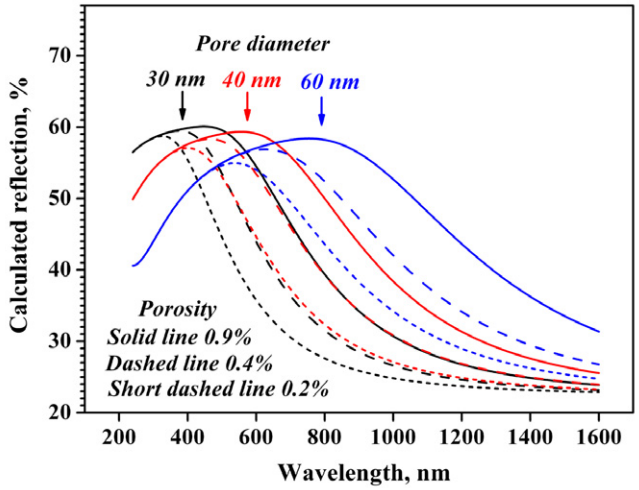

Figure 9. Reflection simulated with the *BHMIE* program for various porosities and pore sizes in the zirconia matrix [7, 11, 20, 22]. The value of reflection was obtained by subtracting the total forward transmittance from 100%.

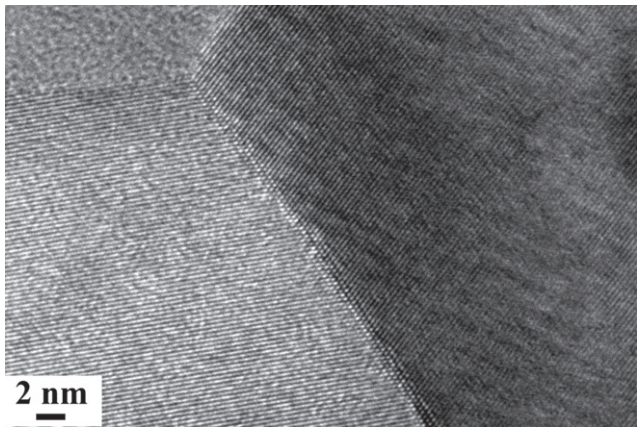

Figure 10. High-resolution TEM image of the grain boundaries in the c-YSZ sintered at 1150 °C for 10 min under a pressure of 400 MPa.

second phases are not observed along the grain boundaries and thus do not contribute to light scattering. Birefringent scattering at grain boundaries is forbidden by symmetry because of the cubic crystal structure of YSZ [10–12]. In addition, the contribution of grain boundaries to the absorption loss can be neglected from experiment and theoretical analysis [10–12], [23, 40, 41]. Therefore, we conclude that the optical properties of sintered zirconia are mostly affected by color centers and residual pores rather than grain boundaries.

4. Conclusions

We have correlated the microstructure and optical properties of the translucent cubic zirconia stabilized by 8 mol% yttria and sintered by high-pressure SPS at a temperature between 1000 and 1200 °C. The optimum sintering temperature of 1100 °C can be explained as follows: at lower temperatures, the densification is low that results in significant light scattering and opaque samples, whereas higher temperatures produce additional absorption and scattering defects. The evolution of total forward and in-line transmittance is mainly controlled by color centers (oxygen vacancies with trapped electrons) generated in the reducing environment of SPS. In our samples, residual pores have only a limited effect on scattering, mostly seen in the ultraviolet region. The reduction of the total forward transmittance and in-line transmittance with sintering temperature is related to the generation of color centers and residual pores. The removal of color centers by annealing in oxidizing atmosphere can improve the total forward transmittance and in-line transmittance despite the increase of porosity. The reflection is only related to the porosity and is enhanced by annealing because of the increasing porosity. The transparency is yet lower for the sintered than single-crystal zirconia due to the presence of color centers, and it can be increased by eliminating these defects. The following improvements might be useful

for achieving this goal: (i) deagglomeration treatment of commercial zirconia powders and (ii) increasing the applied pressure to 600–800 MPa that should allow decreasing the sintering temperature.

Acknowledgment

This work was partly supported by the Grant-in Aid for Scientific Research (C-22560675) from the Ministry of Education, Culture, Sports, Science and Technology, Japan.

References

[1] Vahldiek F W 1967 *J. Less-Common Met.* **13** 530
[2] Mazdiyasni K S, Lynch C T and Smith J S II 1967 *J. Am. Ceram. Soc.* **50** 532
[3] Duran P, Reico P, Jurado J R, Pascual C and Moure C 1989 *J. Am. Ceram. Soc.* **72** 2088
[4] Srdic V V, Winterer M and Hahn H 2000 *J. Am. Ceram. Soc.* **83** 729
[5] Srdic V V, Winterer M and Hahn H 2000 *J. Am. Ceram. Soc.* **83** 1853
[6] Tsukuma K 1986 *J. Mater. Sci. Lett.* **5** 1143
[7] Tsukuma K, Yamashita I and Kusunose T 2008 *J. Am. Ceram. Soc.* **91** 813
[8] Peuchert U, Okano Y, Menke Y, Reichel S and Ikesue A 2009 *J. Eur. Ceram. Soc.* **29** 283
[9] Casolco S R, Xu J and Garay J E 2008 *Scr. Mater.* **58** 516
[10] Alaniz J E, Perez-Gutierrez F G, Aguilar G and Garay J E 2009 *Opt. Mater.* **32** 62
[11] Anselmi-Tamburini U, Woolman J N and Munir Z A 2007 *Adv. Funct. Mater.* **17** 3267
[12] Zhang H B, Kim B N, Morita K, Yoshida H, Lim J H and Hiraga K 2010 *J. Alloys Compd.* **508** 196
[13] Risbud S H, Shan C H, Mukherjee A K, Kim M J, Bow J S and Holl R A 1995 *J. Mater. Res.* **10** 237
[14] Stanciu L A, Kodash V Y and Groza J R 2001 *Metall. Mater. Trans. A* **32** 2633
[15] Zhan G D, Kuntz J, Wan J, Garay J and Mukherjee A K 2002 *Scr. Mater.* **47** 737
[16] Shen Z, Johnsson M, Zhao Z and Nygren M 2002 *J. Am. Ceram. Soc.* **85** 1921
[17] Zhou Y, Hirao K, Yamauchi Y and Kanzaki S 2004 *J. Eur. Ceram. Soc.* **24** 3465
[18] Jiang D T, Hulbert D M, Anselmi-Tamburini U, Ng T, Land D and Mukherjee A K 2008 *J. Am. Ceram. Soc.* **91** 151
[19] Kim B N, Hiraga K, Morita K and Yoshida H 2007 *Scr. Mater.* **57** 607
[20] Kim B N, Hiraga K, Morita K, Yoshida H, Miyazaki T and Kagawa Y 2009 *Acta Mater.* **57** 1319
[21] Kim B N, Hiraga K, Morita K and Yoshida H 2009 *J. Eur. Ceram. Soc.* **29** 323
[22] Kim B N, Hiraga K, Morita K, Yoshida H and Kagawa Y 2010 *Acta Mater.* **58** 4527
[23] Morita K, Kim B N, Hiraga K and Yoshida H 2008 *Scr. Mater.* **58** 1114
[24] Frage N, Cohen S, Meir S, Kalabukhov S and Dariel M P 2007 *J. Mater. Sci.* **42** 3273
[25] Meir S, Kalabukhov S, Froumin N, Dariel M P and Frage N 2009 *J. Am. Ceram. Soc.* **92** 358
[26] Wang C and Zhao Z 2009 *Scr. Mater.* **61** 193
[27] Chaim R, Marder R and Estournes C 2010 *Scr. Mater.* **63** 211
[28] Chaim R, Kalina M and Shen J Z 2007 *J. Eur. Ceram. Soc.* **27** 3331
[29] Chaim R, Marder-Jaeckel R and Shen J Z 2006 *Mater. Sci. Eng.* A **429** 74
[30] Chaim R, Shen Z J and Nygren M 2004 *J. Mater. Res.* **19** 2527
[31] Zhang G M, Wang Y C, Fu Z Y, Wang H, Wang W M, Zhang J Y, Lee S W and Niihara K 2009 *J. Eur. Ceram. Soc.* **29** 2705
[32] Imai T, Naitoh Y, Yamamoto T and Ohyanagi M 2006 *J. Ceram. Soc. Japan* **114** 138
[33] Grasso S, Kim B N, Hu C F, Maizza G and Sakka Y 2010 *J. Am. Ceram. Soc.* **93** 2460
[34] Krell A, Hutzler T and Klimke J 2009 *J. Eur. Ceram. Soc.* **29** 207
[35] Wright D A, Thorp J S, Aypar A and Buckley H P 1973 *J. Mater. Sci.* **8** 876
[36] Savoini B, Ballesteros C, Munoz-Santiuste J E, Gonzalez R and Chen Y 1998 *Phys. Rev.* B **57** 13439–47
[37] Pai-Verneker V R, Petelin A N, Crowne F J and Nagle D C 1989 *Phys. Rev.* B **40** 8555–7
[38] Grasso S, Sakka Y and Maizza G 2009 *Sci. Technol. Adv. Mater.* **10** 053001
[39] Zhang H B, Kim B N, Morita K, Yoshida H, Lim J H and Hiraga K 2011 *J. Am. Ceram. Soc.* at press DOI: 10.1111/j.1551–2916.2011.04477.x
[40] Morita K, Kim B N, Hiraga K and Yoshida H 2009 *J. Mater. Res.* **24** 2863
[41] Morita K, Kim B N, Yoshida H and Hiraga K 2009 *J. Am. Ceram. Soc.* **92** 1208